Received: 8 July 2022 | Revised: 22 October 2022 | Accepted: 27 October 2022

DOI: 10.1002/mgg3.2090

Molecular Genetics & Genomic Medicine Open Access WILEY

ORIGINAL ARTICLE

The compound heterozygous mutations of c.607G>a and c.657delC in the *FAH* gene are associated with renal damage with hereditary tyrosinemia type 1 (HT1)

Huan Chi[1] | **Chun Gan**[1] | **Yaru Jiang**[1] | **Dan Chen**[1] | **Jiawen Qiu**[1] | **Qing Yang**[1] | **Yaxi Chen**[2] | **Mo Wang**[1] | **Haiping Yang**[1] | **Wei Jiang**[1] | **Qiu Li**[1]

[1]Pediatric Research Institute, National Clinical Research Center for Child Health and Disorders, China International Science and Technology Cooperation Base of Child development and Critical Disorders, Chongqing Key Laboratory of Pediatrics, Children's Hospital of Chongqing Medical University, Chongqing, P.R. China

[2]Centre for Lipid Research & Key Laboratory of Molecular Biology for Infectious Diseases (Ministry of Education), Institute for Viral Hepatitis, Department of Infectious Diseases, The Second Affiliated Hospital, Chongqing Medical University, Chongqing, P.R. China

Correspondence
Wei Jiang and Qiu Li, Pediatric Research Institute, National Clinical Research Center for Child Health and Disorders, China International Science and Technology Cooperation Base of Child development and Critical Disorders, Chongqing Key Laboratory of Pediatrics, Children's Hospital of Chongqing Medical University, Chongqing, P.R. China.
Email: jainveborry@163.com and liqiu809@hospital.cqmu.edu.cn

Funding information
Multi-Center Innovation Platform for Early Development and Major Diseases of Perinatal Newborns in Different Altitude Areas; Second Batch of Funds for Chongqing Talents and Famous Teachers, Grant/Award Number: 020210; National Natural Science Foundation of China, Grant/Award Number: 81970618; General Project of Basic Research of Key Laboratory of Ministry of Education for Research on Child Developmental Diseases, Children's Hospital of Chongqing Medical University, Grant/Award Number: GBRP-202111

Abstract

Background: Hereditary tyrosinemia type 1 (HT1) is a rare inherited metabolic disease characterized by severe liver and renal dysfunction. Early identification in affected children is critical for improved treatment options and prognosis.

Methods: In this study, we identified novel compound heterozygous mutations (NM_000137: c.657delC (p.K220Rfs*12) and c.607G>A (p.A203T)) in the *fumarylacetoacetate hydrolase* (*FAH*) gene in a family. We also characterized the clinical phenotype of the proband and verified the pathogenic effects of the mutations. Furthermore, we explored the pathogenic mechanism of renal injury through renal biopsy pathology and cell-based in vitro assays. Our study aims to verify the association between novel fumarylacetoacetate hydrolase (FAH) variants and HT1, confirm the pathogenic effects of the mutations and explore the pathogenic mechanism of renal injury.

Results: We showed these *FAH* mutations were inherited in an autosomal recessive manner and resulted in abnormal FAH protein expression and dysfunction, leading to fumarylacetoacetate (FAA) accumulation. The proband also showed apparent renal injury, including glomerular filtration barrier dysfunction and abnormal tubular protein reabsorption.

Conclusions: These observations may provide deeper insights on disease pathogenesis and identify potential therapeutic approaches for HT1 from a genetic perspective. Similarly, we hope to provide valuable information for genetic counseling and prenatal diagnostics.

This is an open access article under the terms of the Creative Commons Attribution-NonCommercial-NoDerivs License, which permits use and distribution in any medium, provided the original work is properly cited, the use is non-commercial and no modifications or adaptations are made.
© 2022 The Authors. *Molecular Genetics & Genomic Medicine* published by Wiley Periodicals LLC.

KEYWORDS

chronic kidney disease, *fumarylacetoacetate hydrolase*, hereditary tyrosinemia type 1, mutation, whole exome sequencing

1 | INTRODUCTION

Globally, chronic kidney disease (CKD) affects more than 800 million people. While significant improvements in disease therapy have been generated, patients remain at risk for end-stage renal disease (ESRD) (Chapman et al., 2021; Jager et al., 2019). Although our understanding of CKD pathogenesis is incomplete, the analysis of disease-causing mutations in early-onset CKD has provided new insights into disease pathogenesis. Over the past decade, next-generation sequencing (NGS) technologies have revolutionized genetics, with increased access to NGS technologies paving the way for routine genetic testing in genetically heterogeneous kidney diseases (Boyer et al., 2011; Weng et al., 2021).

Using whole exome sequencing (WES), more than 600 causative CKD gene mutations have been identified and exemplify the continued relevance of genetic factors in disease development (Connaughton et al., 2019; Mann et al., 2019; Rao et al., 2019). Hereditary tyrosinemia type 1 (HT1) (OMIM 276700) is a rare autosomal recessive genetic disease caused by a deficiency in fumarylacetoacetate hydrolase (FAH), the last enzyme in the tyrosine breakdown cascade (Figure 1a) (Introne, 2021). Failure to correctly break down tyrosine leads to the abnormal accumulation of toxic metabolites and results in severe liver and kidney damage (Angileri, Bergeron, et al., 2014; Morrow et al., 2017). Thus, deficient enzyme activity leads to the accumulation of the toxic FAH substrate, fumarylacetoacetate (FAA) in hepatocytes and kidney cells. This state is characterized by severe liver failure and proximal renal tubular cells manifesting renal dysfunction which is associated with growth failure and rickets (Angileri, Morrow, et al., 2014; Nakamura et al., 2007).

Extensive research has explored multi-system and multi-organ damage mechanisms in patients with HT1, but this field remains largely unexplored for kidney disease (Awata et al., 1994; Morrow et al., 2017; Tanner, 2002; Van Dyk et al., 2010). Insights on the relationship between gene polymorphisms and amino acid metabolism have helped target *FAH* mutation-mediated tyrosinemia processes underlying renal dysfunction (Angileri, Bergeron, et al., 2014; Dursun et al., 2011; Morrow et al., 2017). Up to now, approximately 100 pathogenic *FAH* variants have been reportedly associated with HT1, and despite

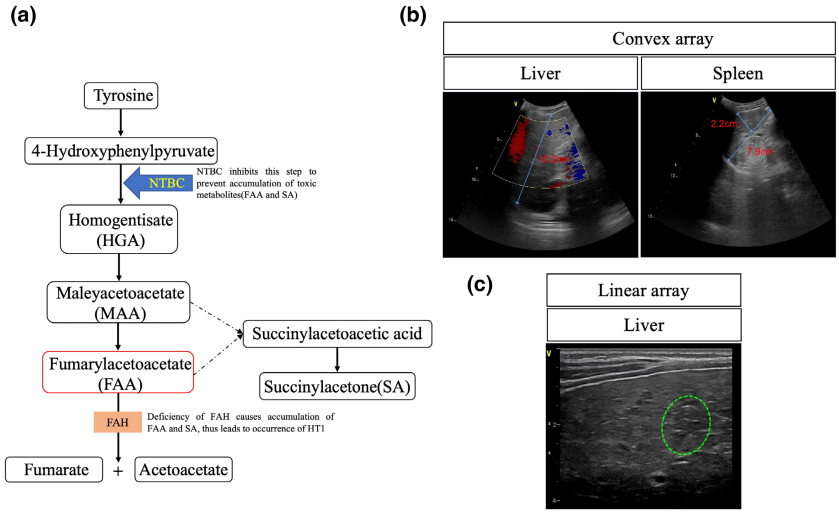

FIGURE 1 Abdominal ultrasonography reveals hepatosplenomegaly in the proband. (a) Tyrosine catabolic pathway. Several enzymes are involved in tyrosine metabolism. 2-(2-Nitro-4-trifluoromethylbenzoyl)-1,3-cyclohexanedione (NTBC) inhibits the enzyme in the second metabolism step to prevent fumarylacetoacetate (FAA) and succinylacetone (SA) toxic metabolite accumulation. FAH catalyzes FAA conversion to fumarate and acetoacetate, with FAH deficiency leading to FAA accumulation and the by-passing of the metabolite SA, which causes hereditary tyrosinemia type 1 (HT1). (b) Convex-array ultrasound images show an enlarged liver; the oblique diameter of the right lobe was 10.2 cm. The spleen was also enlarged (dimensions; 7.9 × 2.2 cm). (c) Linear-array ultrasound image of the liver showed enhanced echo-intensity of the liver parenchyma (annotated by the green circle) and a coarse echotexture of the liver along with heterogeneous echogenicity were observed.

numerous studies, no clear genotype–phenotype map has been established (Angileri, Bergeron, et al., 2014; Baydakova et al., 2019; Ibarra-González et al., 2019). For children with atypical clinical manifestations, the identification of biallelic pathogenic *FAH* variants using molecular genetic testing should be combined, especially for prenatal diagnoses.

Using WES, we identified compound heterozygous mutations (NM_000137: c.657delC (p.K220Rfs*12) and NM_000137: c.607G>A(p.A203T)) in *FAH* in a family associated with HT1. With chronic onset, the proband showed multi-system and multi-organ damage, where liver and renal involvement were most pronounced. Further analyses confirmed the pathogenicity of *FAH* variants and linked them to HT1. Importantly, these variants resulted in the abnormal expression and function of the FAH protein and disorders in tyrosine degradation, which led to severe liver failure accompanied by renal glomerular filtration barrier dysfunction and abnormal protein reabsorption in renal tubules. These findings provide new genetic insights on the pathogenesis and therapeutic approaches for CKD, and may link *FAH* polymorphisms to renal insufficiency. Also, our study provides important information for genetic counseling and prenatal diagnostics.

2 | MATERIALS AND METHODS

2.1 | Ethical compliance

The study followed the principles of the Declaration of Helsinki and was approved by the Ethics Committee of the Children's Hospital of Chongqing Medical University (No. 2021-228).

2.2 | Patient and genetic analysis

The proband was a 38-month-old girl whose clinical data, including demographic information, family history, diagnosis, and laboratory test were collected. DNA extracted from EDTA-treated peripheral blood samples of the proband and her family members using the QIAamp DNA Blood Mini kits (QIAGEN Science) was subjected to whole-exome Illumina sequencing (MyGenostics). Assessment of pathogenicity of the mutations was performed following the American College of Medical Genetics and Genomics (ACMG) guidelines and mutations in *FAH* were confirmed by Sanger sequencing. GRCh37 or hg19 (GenBank accession number: NM_000137.4) was used as the reference sequence.

2.3 | Bioinformatics analysis

ClustalW multiple sequence alignment of FAH protein in several species was achieved by Clustal Omega (https://www.ebi.ac.uk/Tools/msa/clustalo/). Crystal structure of FAH protein was analyzed by the SWISS-MODEL (https://swissmodel.expasy.org).

2.4 | Histological analysis and staining

The patient underwent kidney biopsy at our institution (Children's Hospital of Chongqing Medical University). The decision to biopsy was at the discretion of the attending nephrologist. Core needle biopsy material was examined under the stereomicroscope and divided for light and electron microscopy studies. The sample for light microscopy was fixed in neutral buffered formalin and was embedded in paraffin or optimal cutting temperature (OCT, 4583, SAKURA) compound by using standard procedures (Yamane et al., 2020). Paraffin sections were stained with hematoxylin & eosin (H&E), periodic acid-Schiff staining (PAS), periodic acid-silver metheramine (PASM), Masson, immunohistochemistry (IHC) and immunofluorescence (IF), respectively. Digital images were obtained with a light microscope (Olympus).

2.5 | Transmission electron microscopy (TEM)

Electron microscopic sample handling and detection were performed by the electron microscopic core lab of Chongqing Medical University. The ultrastructure of podocyte foot process was analyzed using Image Pro plus 6.0. Four glomeruli were randomly selected and 10 electron micrographs were taken in each glomerulus.

2.6 | Confocal and fluorescence microscopy

Kidney biopsies and 293T cells fixed in neutral buffered formalin were embedded in paraffin or optimal cutting temperature compound by using standard procedures (LeBleu et al., 2013). Frozen and paraffin sections were stained with immunofluorescence, respectively. Immunofluorescent staining and images were obtained by a Nikon A1R Meta confocal microscope. Coverslips were observed.

The antibodies used were listed below: rabbit polyclonal antibody to Synaptopodin (1:50, 21,064-1-AP,

Proteintech), rabbit monoclonal antibody to Cubilin (1:500, ab191073, Abcam), rabbit polyclonal antibody Megalin antibody (1:30, CD7D5, Novus Biologicals), anti-COL4A3 antibody (1:100, Kingmed), anti-COL4A4 antibody (1:100, Kingmed), anti-COL4A5 antibody (1:100, Kingmed), goat polyclonal secondary antibody to mouse Alexa fluor 488 (1:400, ab150113, Abcam), goat polyclonal secondary antibody to rabbit Alexa fluor 555 (1:400, ab150078, Abcam).

Apoptosis index was detected by One-step TdT-mediated dUTP nick-end labeling (TUNEL) Assay Kit (E-CK-A325, Elabscience).

2.7 | Cell culture

293T cells were maintained in DMEM containing 10%(v/v) fetal bovine serum (FBS, Hyclone, 10,100,147) and 1%(v/v) penicillin/streptomycin (Beyotime, C0222) at 37°C and 5% CO^2 in a humidified atmosphere and passaged every 2–3 days. The concentration of dissolved FAA in the complete cell medium was 1 μg/ml (Yang et al., 2019).

2.8 | Plasmid construction and transient transfection

The plasmid vector pLVX-IRES-ZsGreen1 was digested by EcoR I and a 1257 bp of human *FAH* gene and linearized pLVX-IRES-ZsGreen1 were purified. Then, *FAH* and pLVX-IRES-ZsGreen1 were linked utilizing In-Fusion Cloning (Vazyme, ClonExpress II One Step Cloning Kit, C112) to generate shuttle recombinant plasmids pLVX-IRES-ZsGreen1-FAH. The shuttle plasmid was identified by Sanger sequencing analysis. Site-directed mutagenesis of *FAH* was performed using Mut Express MultiS Fast Mutagenesis Kit V2(Vazyme, C215) and also identified by Sanger sequencing analysis.

The day prior to transfection, the cells were seeded into 6-well plates at 1.2×10^6 cells/well. The cells were transfected using Lipofectamine3000 (Fisher Scientific) according to the manufacturer's instructions with 2500 ng of respective plasmid DNA per well. After 6–7 h, the medium was exchanged with fresh medium.

2.9 | Western blot analysis

For western blotting, whole-cell protein samples were extracted and quantified then boiled at 95°C, 10 min. Then the samples were separated by sodium dodecyl sulfate polyacrylamide gel electrophoresis (SDS-PAGE) and then transferred into a polyvinylidene fluoride (PVDF) membrane and incubated with primary antibodies overnight at 4°C, with specific primary antibodies against FAH (1:500, PA5-42049, Invitrogen), Bax (1:1000, 380709, Zen Bioscience), Bcl2(1:1000, 15071T, Cell Signaling Technology) and GAPDH (TA802519, 1:2000, Origene) in Tris-Buffered Saline Tween-20 (TBST) containing 5% skim milk. After washed for three times with TBST, the membranes were incubated for 1 h at room temperature with a respective IgG-HRP labeled second antibody (1:3000) in TBST. Antigens were revealed using a chemiluminescence assay (Pierce ECL Western Blotting Substrate, 32209, Thermo) and quantification of bands was achieved by densitometry using the Image J software.

2.10 | Statistical analyses

All data were analyzed using GraphPad Prism 7 (Macintosh). Quantitative values are presented as the mean ± SD. For multiple comparison analysis, one-way ANOVA followed by Tukey's multiple comparison tests was performed.

3 | RESULTS

3.1 | Correlation between the clinical phenotypes of the child and HT1

The proband was a 38-month-old female having disease onset at 2 years old, and mainly manifested with recurrent proteinuria, macroscopic hematuria, and hepatosplenomegaly, without a clear trigger. The clinical characteristics of the patient are shown (Table 1). The conventional liver dysfunction biochemical markers, serum aspartate transaminase (AST), and alkaline phosphatase (ALP) were elevated. Abdominal ultrasounds revealed hepatosplenomegaly (Figure 1b). In addition, echo-intensity of the liver parenchyma was enhanced and a coarse echotexture of the liver along with heterogeneous echogenicity was observed (Figure 1c). The tandem mass spectrum showed increased tyrosine and SA levels in the blood and urine. The proband's parents and younger sister appeared healthy. Given these clinical findings, presenting as unknown renal/liver dysfunction and abnormal tyrosine metabolic pathway function (Figure 1a), we suspected an inherited metabolic disease and finally HT1 was considered.

TABLE 1 Clinical characteristics of patient

Clinical, biochemical, and immunological parameters	Reference range	Result
Clinical		
Age at symptoms onset (months)	—	24
Classification	—	Chronic
Age at diagnosis (months)	—	38
Hepatosplenomegaly	—	Yes
Proteinuria	—	Yes
Gross hematuria	—	Yes
Biochemical		
Tyrosine (μmol/L)	20.00–120.00	209.97 ↑
Succinylacetone-OX-2(1) of urine	0.0–0.0	49.1 ↑
Succinylacetone of blood (μmol/L)	≤2.0	7.3 ↑
AST (U/L)	0–45	77.3 ↑
ALP (U/L)	100–360	502 ↑
BUN (mmol/L)	2.42–6.72	5.23
Scr (μmol/L)	15.4–90.4	20
SUA (μmol/L)	140–390	157
PT (s)	9.0–14	14.7 ↑
Immunological parameters		
IgG (g/L)	2.86–16.8	7.16
IgA (g/L)	0.22–2.2	0.408
IgM (g/L)	0.43–1.63	1.22
IgE (IU/ml)	0–165	19.3
C3 (g/L)	0.7–2.06	0.66 ↓
C4 (g/L)	0.11–0.61	0.08 ↓

Note: The proband presented with multi-organ damage.

Abbreviations: ALP, alkaline phosphatase; AST, serum aspartate transaminase; BUN, blood urea nitrogen; C3, complement component 3; C4, complement component 4; IgA, immunoglobulin A; IgE, immunoglobulin E; IgG, immunoglobulin G; IgM, immunoglobulin M; PT, prothrombin time; Scr, serum creatinine; SUA, serum uric acid.

3.2 | The identification of compound heterozygous mutations (c.657delC(p.K220Rfs*12), c.607G>a(p.A203T)) in *FAH*

Even when factors commonly associated with disease were evaluated, uncertainty remained regarding some of the proband's clinical phenotypes, which may suggest the pathogenic effect of genetic factors. To this end, after considering the proband's unexplained liver and kidney dysfunction and abnormal tyrosine metabolism with genetic heterogeneity, we adopted a molecular approach and performed WES on the family members to determine a molecular diagnosis. Subsequently, genetic analyses detected compound heterozygous mutations in *FAH* (c.657delC(p.K220Rfs*12)) and c.607G>A(p. Alanine 203 to Threonine, A203T), with both variants verified by Sanger sequencing (Figure 2a). In light of the genetic predisposition, Sanger sequencing of the proband's parents, who did not exhibit any clinically pathogenic phenotypes, confirmed both were asymptomatic heterozygous carriers for the compound mutations (Figure 2b).

To predict mutation pathogenicity, we accessed several online tools, including American College of Medical Genetics (ACMG), Rare Exome Variant Ensemble Learner (REVEL), Sorting Intolerant From Tolerant (SIFT), PolyPhen2, Mutation Taster, and Genomic Evolutionary Rate Profiling (GERP). These tools showed that the c.657delC (p.K220Rfs*12) mutation was annotated as likely pathogenic and the c.607G>A(p.A203T) mutation may lead to damaged function of protein (Table 2). To detect the effects of the c.607G>A (p.A203T) variant on FAH protein function, we performed amino acid conservation analysis on the missense FAH variant site (p.A203T) by ClustalW multiple sequence alignments. Interestingly, the 203rd residue, alanine was highly conserved across multiple species (Figure 2c). Also, three-dimensional structural models showed that both variants may have altered FAH folding and function (Figure 2d). Accordingly, these mutations may have affected liver and kidney function.

3.3 | *FAH* mutations target FAH expression and function

To further elucidate whether these mutations affected FAH expression or function, recombinant wild type (WT) FAH, FAH (c.607G>A), and FAH (c.657delC) plasmids were constructed and transiently transfected into human embryonic kidney (HEK) 293T cells. Western blotting (WB) showed that FAH expression in FAH (c.657delC) transiently transfected cells was decreased while FAH (c.607G>A (p.A203T)) expression was similar to FAH (WT) cells (Figure 3a), suggesting the c.657delC (p.K220Rfs*12) mutation impacted FAH expression. To investigate the effects of variants on the regulation of FAA-induced apoptosis, we analyzed expression of the apoptosis-related markers, Bax and Bcl2 using WB. Our data indicated significantly increased Bax expression and decreased Bcl-2 expression in c.607G>A (p.A203T) cells (Figure 3b). Similar data were obtained from terminal deoxynucleotidyl transferase (TdT)-mediated dUTP nick end labeling (TUNEL) assays (Figure 3c). Moreover, FAH immunohistochemistry on proband kidney biopsies showed a marked decline in FAH expression when compared with healthy controls (HCs, adjacent normal kidney tissue samples) (Figure 3d). Thus, these mutations targeted FAH expression and function resulting in apoptosis mediated by the mitochondria.

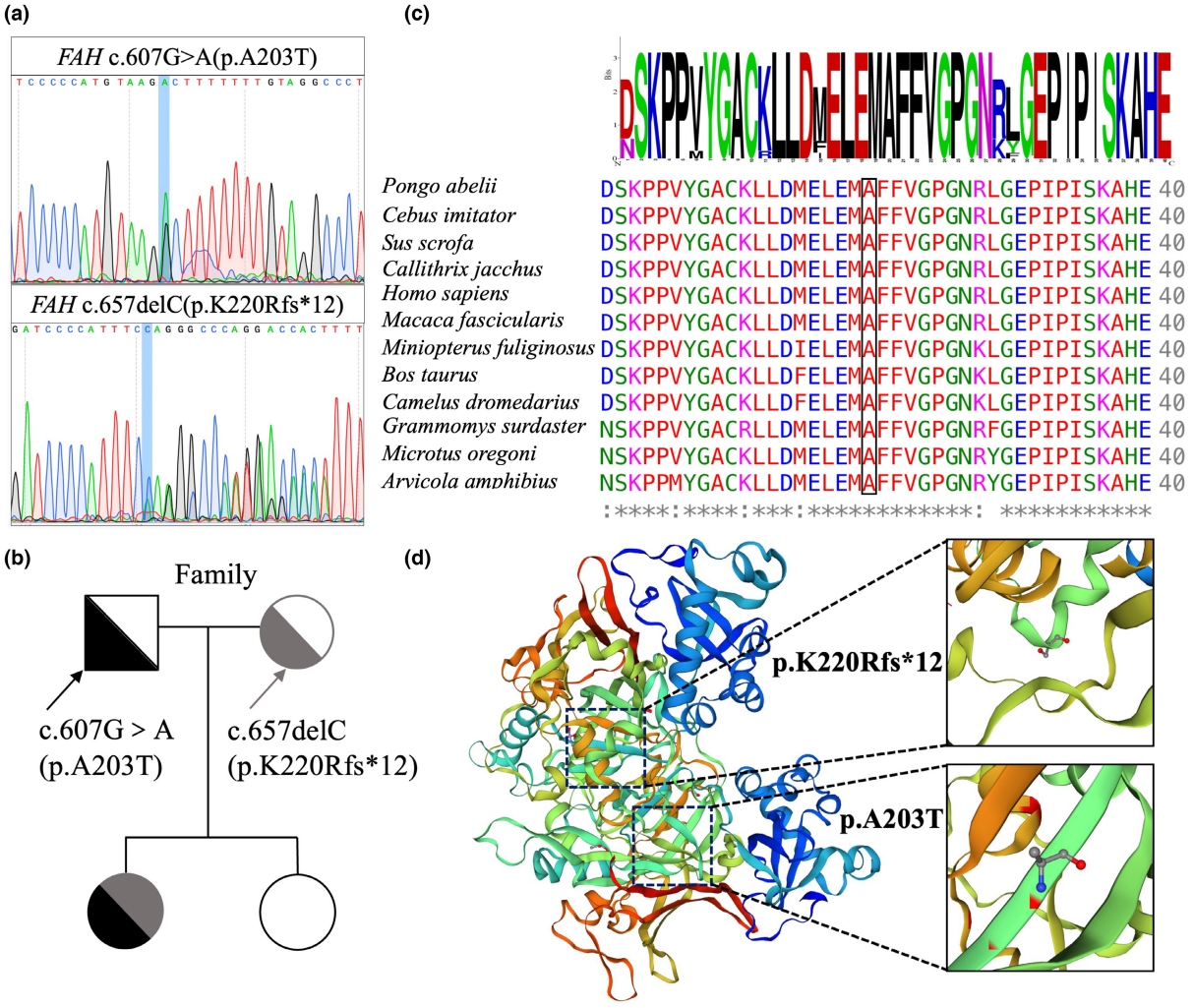

FIGURE 2 The identification of compound heterozygous mutations in *FAH* using whole-exome sequencing (WES) in the proband's family. (a) WES identified the *FAH* variants: c.657delC and c.607G>a which were confirmed by Sanger sequencing. (b) The family pedigree; squares = male subjects; circles = female subjects. (c) ClustalW multiple sequence alignment of the FAH protein across several species. The missense mutation (p.A203T) in the proband was located at a highly conserved position in the FAH protein (black box). Asterisks below the sequence alignment indicate an evolutionary conserved residue. The colon indicates a highly conserved residue and the period represents less conserved residues. (d) Mutant FAH tertiary protein structures were modeled using SWISS-MODEL. Mutation of the amino acid residues, p.A203T and p.K220Rfs*12 are marked on the molecular structure.

3.4 | *FAH* mutations may be related to renal damage

To identify the impact of mutations on renal tissue injury, we investigated pathological kidney changes in the proband using H&E, PAS, PASM, and Masson in renal sections. Mesangial hyperplasia, glomerulosclerosis, or segmental sclerosis were not observed and the capillary loops of the glomerulus were well-defined and thin (Figure 4a). Also, no obvious tubular atrophy or vacuolar changes were observed (Figure 4a). Immunofluorescence (IF) staining for COL4A3, COL4A4, and COL4A5, which are major components of the glomerular basement membrane (GBM) and reflect glomerular filtration function, showed this structure was intact (Figure 4b). To further examine renal morphology, transmission electron microscopy (TEM) showed podocyte foot process fusion was accompanied by crumpled GBMs and mesangial electron-dense deposits (Figure 4c). Hence, these morphological abnormalities, mediated by *FAH* mutations, may have been related to the renal damage in this patient.

3.5 | *FAH* mutations contribute to proteinuria occurrence and development

Given our discovery that *FAH* mutations could cause renal dysfunction, we explored possible reasons for the recurrent proteinuria in our patient. Thus, we focused on glomerular filtration barrier and tubular reabsorption

functions using IF on synaptopodin (synpo) which is a key podocyte marker, and Cubilin and Megalin which are essential proteins involved in the tubular reabsorption of peptides from glomerular ultrafiltrates (Amsellem et al., 2010; Kozyraki & Cases, 2020). We showed that the staining patterns of these proteins were discontinuous in nature when compared with normal kidney tissue (Figure 4d,e), indicating glomerular filtration barrier impairment and tubular reabsorption dysfunction.

Collectively, these observations showed that the *FAH* mutations, leading to renal insufficiency, presented as dysfunctional glomerular structures and renal tubular protein reabsorption, thereby contributing to proteinuria occurrence and development.

3.6 | Review of the literatures about *FAH* mutations associated with HT1

A retrospective analysis and literature reviews had been performed to determine the final outcome of the patient. To date, over 900 mutations of *FAH* have been identified. Among them, around 100 variants were reported to be associated with HT1 (Table S1) (Angileri et al., 2015; Angileri, Bergeron, et al., 2014; Angileri, Morrow, et al., 2014; Awata et al., 1994; Baydakova et al., 2019; Bergman et al., 1998; Couce et al., 2011; Dursun et al., 2011; Forget et al., 1999; Gokay et al., 2016; Ibarra-González et al., 2019; Imtiaz et al., 2011; Introne, 2021; Kawabata et al., 2022; Luijerink et al., 2004; Maiorana et al., 2014; McKiernan et al., 2015; Morrow et al., 2017; Morrow et al., 2019; Nakamura et al., 2007; Pérez-Carro et al., 2014; Ploos van Amstel et al., 1996; Van Dyk et al., 2010; van Spronsen et al., 1994; Wu & Hurst, 2016). It was worth noting that the most frequent *FAH* mutation to cause HT1 is c.1062+5G>A (IVS12+5G>A) (32.3%), followed by c.554-1G>T (IVS6-1G>T) (16.4%) and c.786G>A (p.W262X) (5.6%) (Angileri, Bergeron, et al., 2014). However, previously identified variants were mainly distributed near the 5′ and 3′ ends of coding sequence (CDS), while the novel variants in our study were located in the middle region of CDS. Meanwhile, functional studies on associations of variants in *FAH* and HT1 suggested decreased expression and functional impairment of FAH protein, exhibiting revealed abnormal FAH expression caused by c.657delC (p.K220Rfs*12) as well as the abnormal function of FAH caused by c.607G>A(p.A203T). Having been diagnosed with HT1, an urgent need for the proband to receive an optimal treatment regimen was essential to induce remission of HT1. Fortunately, treatment with 2-(2-Nitro-4-trifluoro methylbenzoyl)-1,3-cyclohexanedione (NTBC) combined with a low tyrosine/phenylalanine diet is currently a mainstay treatment for

TABLE 2 *FAH* variants in the proband

FAH gene location	cDNA sequence variation (NM_000137.2)	Protein variant	Hom/het	Pathogenicity prediction	Classification according to ACMG	Disease (mode of inheritance)	Source of variation
Exon 8	c.657delC	p.K220Rfs*12	het	Uncertain	Likely pathogenic	HT1(AR)	Mother
Exon 8	c.607G>A	p.A203T	het	Damage	Uncertain	HT1(AR)	Father

Note: Both mutation sites were located on exon 8 of *FAH* (reference sequence: GRCh37; GenBank accession number: NM_000137.4). c.657delC(p.K220Rfs*12) was annotated as likely pathogenic using ACMG, and c.607G>a(p.A203T) was predicted by several pathogenicity prediction packages, including REVEL, SIFT, PolyPhen2, mutation taster, and GERP to assess protein function damage.

Abbreviations: ACMG, American College of Medical Genetics; GERP, genomic evolutionary rate profiling; het, heterozygosis; Hom, homozygosis; HT1, hereditary tyrosinemia type 1; SIFT, sorting intolerant from tolerant.

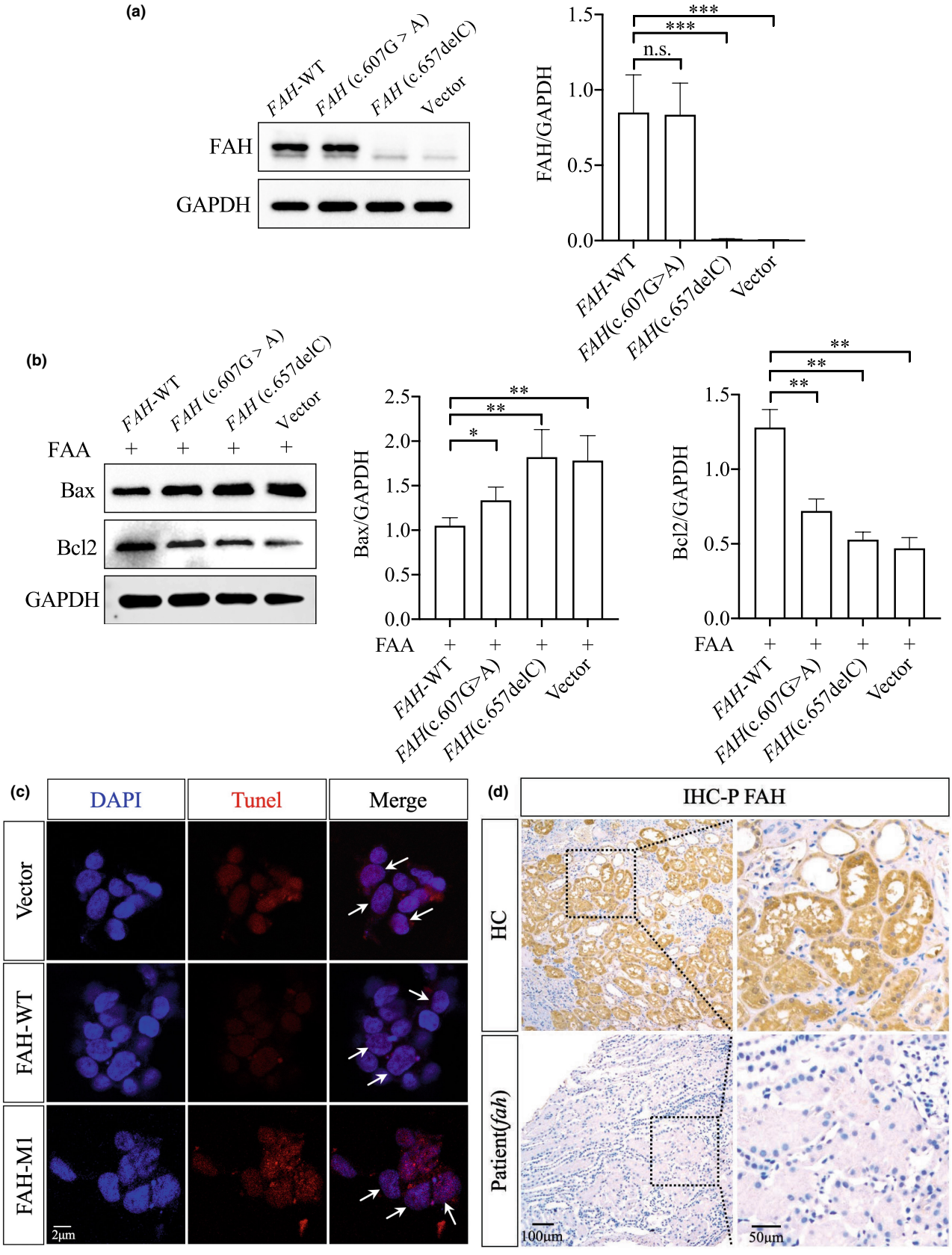

FIGURE 3 Mutations in *FAH* target FAH expression and function. (a) Western blot analysis of FAH protein expression. Expression levels were reduced in c.657delC cells when compared with wild-type (WT) and c.607G>A cells. (b) Western blot analysis of Bax and Bcl2 protein expression during FAA (1 μg/ml) stimulation. Bax expression was increased, while Bcl2 expression was decreased in FAH c.607G>A cells compared to WT cells. (c) Representative TUNEL staining images (blue = DAPI; red = TUNEL). (d) Immunohistochemical (IHC) analysis of FAH in a kidney biopsy from the proband. A significant decline in FAH expression was observed when compared with healthy controls (HCs). For statistical analyses, data are presented as the mean ± standard deviation (SD). n.s, not significant; $^{*}p < 0.05$; $^{**}p < 0.01$.

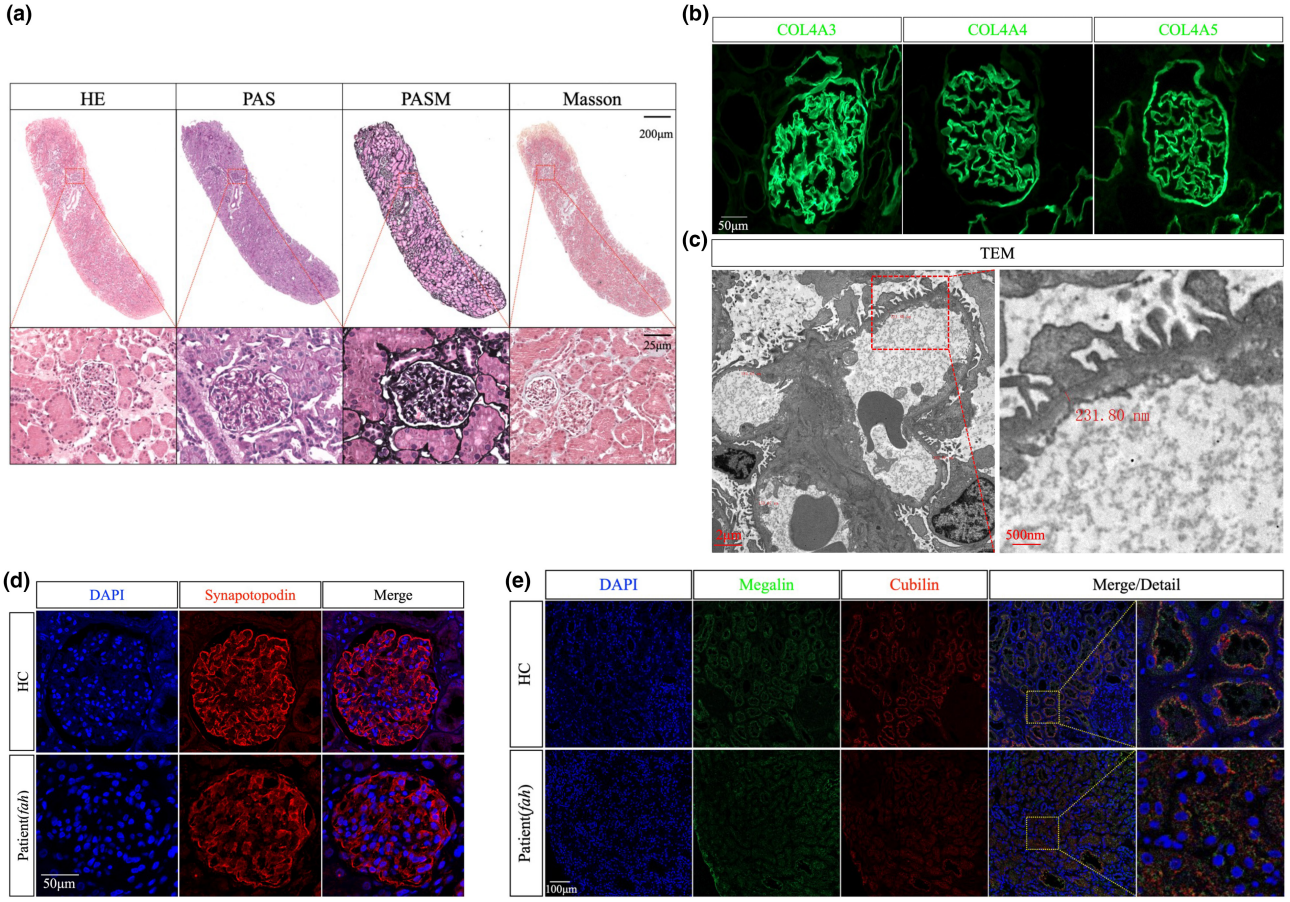

FIGURE 4 The *FAH* mutations may be related to renal dysfunction contributing to proteinuria occurrence and development. (a) Renal biopsies showing hematoxylin–eosin (H&E), periodic acid-Schiff (PAS), periodic acid-silver-meth-enamine (PASM), and Masson staining indicate renal tissue pathology. (b) Immunofluorescence (IF) staining of COL4A3, COL4A4, and COL4A5 showing unimpaired glomerular basement membrane (GBM) structures. (c) Transmission electron microscopy (TEM) images of a proband kidney biopsy, showing foot process fusion accompanied with crumpled GBMs and mesangial electron-dense deposits. (d) Immunofluorescence (IF) staining of synaptopodin (synpo) showing impaired normal linear structures (blue = DAPI; red = synaptopodin). (e) Cubilin and Megalin IF staining showing impaired linear structures (blue = DAPI; green = Megalin; red = Cubilin).

HT1(Angileri, Morrow, et al., 2014), which has improved the prognosis of HT1, and compliance is good. Before a widely applicable utility of NTBC, liver transplantation (LT) with dietary restriction was the primary treatment modalities for HT1.

4 | DISCUSSION

As a rare hereditary metabolic disorder, HT1 significantly impacts on early childhood development, and if effective therapy is lacking, the condition is usually fatal due to hepatic failure, neurological crisis, or hepatocellular carcinoma (Gokay et al., 2016; van Spronsen et al., 1994). Given its damage to the kidneys, HT1 is also an important cause of renal dysfunction, which correlates with a striking increase in CKD and ESRD, without intervention (Maiorana et al., 2014).

The literatures on *FAH* mutations associated with HT1 were systematically reviewed to characterize the associated clinical features in our study. Around 100 variants in *FAH* were reported to be associated with HT1, with a predominance of missense mutations. Exons 9 and 12 of *FAH* gene have the largest clusters of HT1 disease-causing mutations. Interestingly, both of these exons contain metal and substrate-binding sites (Morrow et al., 2017). Additionally, up to now, over 20 *FAH* mutations associated with HT1 phenotype have been reported to affect splicing while some of them do not alter core sequence elements of splicing, they are probably modifying exonic splicing enhancers (ESE) or silencers (ESS) sites and it was shown that 20%–45% of pathogenic single nucleotide polymorphisms (SNPs) affect splicing (Wu & Hurst, 2016). It was thereby inferred that other HT1 causing mutations may affect splicing. Instead, the novel variants in our study located in the middle region

of CDS and resulted in abnormal FAH protein expression and dysfunction, respectively. HT1 is classified in three different forms depending on the clinical phenotype of patients and the age of onset. The acute form presents before 2 months of age with acute liver failure, while the sub-acute form presents between 2 and 6 months of age with liver disease and the chronic form presents after 6 months of age with slowly progressive liver cirrhosis and hypophosphatemic rickets. Multiple researches had tried to explore the relationship between genotype and phenotype of HT1. Couce et al. (2011) described a correlation between low frequency of nephrocalcinosis and IVS6-1(G>T) mutation in 34 Spanish patients with HT1. Despite those efforts, no clear genotype–phenotype relationships have been unveiled. Regardless of the phenotype (acute, subacute, chronic), early administration of NTBC could help to improve the prognosis of HT1. Moreover, even in cases without LT treatment, clinicians should follow up their outcomes for an extended period, and they may need LT when developing complications (Kawabata et al., 2022). For the patient in this study, LT as well as NTBC are being actively pursued, and regular assessment of the current status of the disease as well as treatment outcomes are needed in the near future.

Previous studies confirmed a central role for apoptosis in cellular damage induced by FAA (Angileri et al., 2015; Luijerink et al., 2004), the primary toxic metabolite resulting from FAH deficiency. Similarly, we demonstrated that these mutations failed to degrade FAA. Moreover, we also evaluated renal dysfunction caused by these variants. It is worth noting that renal biopsy analyses in patients with HT1 have been scarcely reported (Forget et al., 1999). We observed abnormal FAH expression in the kidney which was accompanied by glomerular filtration barrier injury and impaired renal tubular function, even though histological changes were relatively mild. Also, proteinuria, as observed in the proband, is considered not only a marker of glomerular damage but also a nephrotoxic factor in renal tubuli (Liu et al., 2014). It is accepted that podocyte impairment and renal tubule injury lead to proteinuria and contribute to the development and progression of proteinuric kidney disease (Araki et al., 2013; Grahammer et al., 2013). Accordingly, we hypothesized that these *FAH* mutations contributed to proteinuria occurrence and development by disturbing the normal functions of glomerular filtration and tubular reabsorption.

In summary, the novel compound heterozygous mutations, NM_000137: c.607G>A (p.A203T) and c.657delC (p.K220Rfs*12) in *FAH* were implicated in HT1 pathogenesis and disrupted FAH protein expression and function. Such consequences not only affected liver function but also caused renal damage by impairing the glomerular filtration barrier and affecting tubular reabsorption. Our findings exemplify the impact of genetic analyses on CKD pathogenesis and the identification of novel therapeutic approaches and expand the pathogenic mutation spectrum of *FAH*. Also, we provide new information for clinical research, genetic counseling, and prenatal diagnostics.

ACKNOWLEDGMENTS

The authors thank the proband and her family for participation in this study. We also thank the doctors, nurses, and other healthcare providers in the Department of Nephrology at Children's Hospital of Chongqing Medical University. Special thanks to the urology and nephropathy center of the Second Affiliated Hospital of Chongqing Medical University for providing adjacent normal kidney tissue samples. This study was supported by grants from the Multi-Center Innovation Platform for Early Development and Major Diseases of Perinatal Newborns in Different Altitude Areas (Special Funds for The Central Government to Guide Local Scientific and Technological Development), the Second Batch of Funds for Chongqing Talents and Famous Teachers (No. 020210), the National Natural Science Foundation of China (No. 81970618) and the General Project of Basic Research of Key Laboratory of Ministry of Education for Research on Child Developmental Diseases, Children's Hospital of Chongqing Medical University (No. GBRP-202111).

CONFLICT OF INTEREST

The authors declare that the research was conducted in the absence of any commercial or financial relationships that could be construed as a potential conflict of interest.

ORCID

Qiu Li https://orcid.org/0000-0002-2481-7168

REFERENCES

Amsellem, S., Gburek, J., Hamard, G., Nielsen, R., Willnow, T. E., Devuyst, O., Nexo, E., Verroust, P. J., Christensen, E. I., & Kozyraki, R. (2010). Cubilin is essential for albumin reabsorption in the renal proximal tubule. *Journal of the American Society of Nephrology: JASN*, *21*(11), 1859–1867.

Angileri, F., Bergeron, A., Morrow, G., Lettre, F., Gray, G., Hutchin, T., Ball, S., & Tanguay, R. M. (2014). Geographical and ethnic distribution of mutations of the fumarylacetoacetate hydrolase gene in hereditary tyrosinemia type 1. *JIMD Reports*, *19*, 43–58.

Angileri, F., Morrow, G., Roy, V., Orejuela, D., & Tanguay, R. (2014). Heat shock response associated with hepatocarcinogenesis in a murine model of hereditary tyrosinemia type I. *Cancers*, *6*(2), 998–1019.

Angileri, F., Roy, V., Morrow, G., Scoazec, J. Y., Gadot, N., Orejuela, D., & Tanguay, R. M. (2015). Molecular changes associated with chronic liver damage and neoplastic lesions in a murine model of hereditary tyrosinemia type 1. *Biochimica et Biophysica Acta*, *1852*(12), 2603–2617.

Araki, S., Haneda, M., Koya, D., Sugaya, T., Isshiki, K., Kume, S., Kashiwagi, A., Uzu, T., & Maegawa, H. (2013). Predictive effects of urinary liver-type fatty acid–binding protein for deteriorating renal function and incidence of cardiovascular disease in type 2 diabetic patients without advanced nephropathy. *Diabetes Care*, *36*(5), 1248–1253.

Awata, H., Endo, F., Tanoue, A., Kitano, A., Nakano, Y., & Matsuda, I. (1994). Structural organization and analysis of the human fumarylacetoacetate hydrolase gene in tyrosinemia type I. *Biochimica et Biophysica Acta (BBA)-Molecular Basis of Disease*, *1226*(2), 168–172.

Baydakova, G. V., Ivanova, T. A., Mikhaylova, S. V., Saydaeva, D. K., Dzhudinova, L. L., Akhlakova, A. I., Gamzatova, A. I., Bychkov, I. O., & Zakharova, E. Y. (2019). The unique Spectrum of mutations in patients with hereditary tyrosinemia type 1 in different regions of The Russian Federation. *JIMD Reports*, *45*, 89–93.

Bergman, A. J., van den Berg, I. E., Brink, W., Poll-The, B. T., Ploos van Amstel, J., & Berger, R. (1998). Spectrum of mutations in the fumarylacetoacetate hydrolase gene of tyrosinemia type 1 patients in northwestern Europe and Mediterranean countries. *Human Mutation*, *12*(1), 19–26.

Boyer, O., Nevo, F., Plaisier, E., Funalot, B., Gribouval, O., Benoit, G., Cong, E. H., Arrondel, C., Tête, M. J., Montjean, R., Richard, L., Karras, A., Pouteil-Noble, C., Balafrej, L., Bonnardeaux, A., Canaud, G., Charasse, C., Dantal, J., Deschenes, G., … Mollet, G. (2011). INF2 mutations in Charcot–Marie–tooth disease with glomerulopathy. *New England Journal of Medicine*, *365*(25), 2377–2388.

Chapman, F. A., Nymanu, D., Maguire, J. J., Davenport, A. P., Newby, D. E., & Dhaun, N. (2021). The therapeutic potential of apelin in kidney disease. *Nature Reviews Nephrology*, *17*(12), 840–853.

Connaughton, D. M., Kennedy, C., Shril, S., Mann, N., Murray, S. L., Williams, P. A., Conlon, E., Nakayama, M., van der Ven, A. T., Ityel, H., Kause, F., Kolvenbach, C. M., Dai, R., Vivante, A., Braun, D. A., Schneider, R., Kitzler, T. M., Moloney, B., Moran, C. P., … Hildebrandt, F. (2019). Monogenic causes of chronic kidney disease in adults. *Kidney International*, *95*(4), 914–928.

Couce, M. L., Dalmau, J., del Toro, M., Pintos-Morell, G., Aldámiz-Echevarría, L., & Spanish Working Group on Tyrosinemia type1 Spanish Working Group on Tyrosinemia type 1. (2011). Tyrosinemia type 1 in Spain: Mutational analysis, treatment and long-term outcome. *Pediatrics International*, *53*(6), 985–989.

Dursun, A., Ozgül, R. K., Sivri, S., Tokatlı, A., Güzel, A., Mesci, L., Kılıç, M., Aliefendioglu, D., Özçay, F., Gündüz, M., & Coşkun, T. (2011). Mutation spectrum of fumarylacetoacetase gene and clinical aspects of tyrosinemia type I disease. *JIMD Reports*, *1*, 17–21.

Forget, S., Patriquin, H. B., Dubois, J., Lafortune, M., Merouani, A., Paradis, K., & Russo, P. (1999). The kidney in children with tyrosinemia: Sonographic, CT and biochemical findings. *Pediatric Radiology*, *29*(2), 104–108.

Gokay, S., Ustkoyuncu, P. S., Kardas, F., & Kendirci, M. (2016). The outcome of seven patients with hereditary tyrosinemia type 1. *Journal of Pediatric Endocrinology & Metabolism: JPEM*, *29*(10), 1151–1157.

Grahammer, F., Schell, C., & Huber, T. B. (2013). The podocyte slit diaphragm—From a thin grey line to a complex signalling hub. *Nature Reviews Nephrology*, *9*(10), 587–598.

Ibarra-González, I., Fernández-Lainez, C., Alcántara-Ortigoza, M. A., González-del Angel, A., Fernández-Henández, L., Guillén-López, S., Belmont-Martínez, L., López-Mejía, L., Varela-Fascinetto, G., & Vela-Amieva, M. (2019). Mutational spectrum of Mexican patients with tyrosinemia type 1: In silico modeling and predicted pathogenic effect of a novel missense FAH variant. *Molecular Genetics & Genomic Medicine*, *7*(12), e937.

Imtiaz, F., Rashed, M. S., Al-Mubarak, B., Allam, R., El-Karaksy, H., Al-Hassnan, Z., Al-Owain, M., Al-Zaidan, H., Rahbeeni, Z., Qari, A., & Meyer, B. F. (2011). Identification of mutations causing hereditary tyrosinemia type I in patients of middle eastern origin. *Molecular Genetics and Metabolism*, *104*(4), 688–690.

Introne, W. J. (2021). Nitisinone: Two decades treating hereditary tyrosinaemia type 1. *The Lancet Diabetes & Endocrinology*, *9*(7), 409–411.

Jager, K. J., Kovesdy, C., Langham, R., Rosenberg, M., Jha, V., & Zoccali, C. (2019). A single number for advocacy and communication—Worldwide more than 850 million individuals have kidney diseases. *Nephrology Dialysis Transplantation*, *34*(11), 1803–1805.

Kawabata, K., Kido, J., Yoshida, T., Matsumoto, S., & Nakamura, K. (2022). A case report of two siblings with hypertyrosinemia type 1 presenting with hepatic disease with different onset time and severity. *Molecular Genetics and Metabolism Reports*, *32*, 100892.

Kozyraki, R., & Cases, O. (2020). Cubilin, the intrinsic factor-vitamin B12 receptor in development and disease. *Current Medicinal Chemistry*, *27*(19), 3123–3150.

LeBleu, V. S., Teng, Y., O'Connell, J. T., Charytan, D., Müller, G. A., Müller, C. A., Sugimoto, H., & Kalluri, R. (2013). Identification of human epididymis protein-4 as a fibroblast-derived mediator of fibrosis. *Nature Medicine*, *19*(2), 227–231.

Liu, W. J., Luo, M. N., Tan, J., Chen, W., Huang, L. Z., Yang, C., Pan, Q., Li, B., & Liu, H. F. (2014). Autophagy activation reduces renal tubular injury induced by urinary proteins. *Autophagy*, *10*(2), 243–256.

Luijerink, M. C., van Beurden, E. A., Malingré, H. E., Jacobs, S. M., Grompe, M., Klomp, L. E., Berger, R., & van den Berg, I. E. T. (2004). Renal proximal tubular cells acquire resistance to cell death stimuli in mice with hereditary tyrosinemia type 1. *Kidney International*, *66*(3), 990–1000.

Maiorana, A., Malamisura, M., Emma, F., Boenzi, S., di Ciommo, V. M., & Dionisi-Vici, C. (2014). Early effect of NTBC on renal tubular dysfunction in hereditary tyrosinemia type 1. *Molecular Genetics and Metabolism*, *113*(3), 188–193.

Mann, N., Braun, D. A., Amann, K., Tan, W., Shril, S., Connaughton, D. M., Nakayama, M., Schneider, R., Kitzler, T. M., van der Ven, A. T., Chen, J., Ityel, H., Vivante, A., Majmundar, A. J., Daga, A., Warejko, J. K., Lovric, S., Ashraf, S., Jobst-Schwan, T., … Hildebrandt, F. (2019). Whole-exome sequencing enables a precision medicine approach for kidney transplant recipients. *Journal of the American Society of Nephrology: JASN*, *30*(2), 201–215.

McKiernan, P. J., Preece, M. A., & Chakrapani, A. (2015). Outcome of children with hereditary tyrosinaemia following newborn screening. *Archives of Disease in Childhood*, *100*(8), 738–741.

Morrow, G., Angileri, F., & Tanguay, R. M. (2017). Molecular aspects of the FAH mutations involved in HT1 disease. *Hereditary Tyrosinemia*, *959*, 25–48.

Morrow, G., Dreumont, N., Bourrelle-Langlois, M., Roy, V., & Tanguay, R. M. (2019). Presence of three mutations in the

fumarylacetoacetate hydrolase gene in a patient with atypical symptoms of hereditary tyrosinemia type I. *Molecular Genetics and Metabolism*, *127*(1), 58–63.

Nakamura, K., Tanaka, Y., Mitsubuchi, H., & Endo, F. (2007). Animal models of tyrosinemia. *The Journal of Nutrition*, *137*(6), 1556S–1560S.

Pérez-Carro, R., Sánchez-Alcudia, R., Pérez, B., Navarrete, R., Pérez-Cerdá, C., Ugarte, M., & Desviat, L. R. (2014). Functional analysis and in vitro correction of splicing FAH mutations causing tyrosinemia type I. *Clinical Genetics*, *86*(2), 167–171.

Ploos van Amstel, J. K., Bergman, A. J., van Beurden, E. A., Roijers, J. F., Peelen, T., Van den Berg, I. E., Kvittingen, E. A., & Berger, R. (1996). Hereditary tyrosinemia type 1: Novel missense, nonsense and splice consensus mutations in the human fumarylacetoacetate hydrolase gene; variability of the genotype-phenotype relationship. *Human Genetics*, *97*(1), 51–59.

Rao, J., Liu, X., Mao, J., Tang, X., Shen, Q., Li, G., Sun, L., Bi, Y., Wang, X., Qian, Y., Wu, B., Wang, H., Zhou, W., Ma, D., Zheng, B., Shen, Y., Chen, Z., Luan, J., Wang, X., … for "Internet Plus" Nephrology Alliance of National Center for Children's Care. (2019). Genetic spectrum of renal disease for 1001 Chinese children based on a multicenter registration system. *Clinical Genetics*, *96*(5), 402–410.

Tanner, M. S. (2002). Mechanisms of liver injury relevant to pediatric hepatology. *Critical Reviews in Clinical Laboratory Sciences*, *39*(1), 1–61.

Van Dyk, E., Steenkamp, A., Koekemoer, G., & Pretorius, P. J. (2010). Hereditary tyrosinemia type 1 metabolites impair DNA excision repair pathways. *Biochemical and Biophysical Research Communications*, *401*(1), 32–36.

van Spronsen, F. J., Thomasse, Y., Smit, G. P., et al. (1994). Hereditary tyrosinemia type I: A new clinical classification with difference in prognosis on dietary treatment. *Hepatology (Baltimore, MD)*, *20*(5), 1187–1191.

Weng, P. L., Majmundar, A. J., Khan, K., Lim, T. Y., Shril, S., Jin, G., Musgrove, J., Wang, M., Ahram, D. F., Aggarwal, V. S., Bier, L. E., Heinzen, E. L., Onuchic-Whitford, A. C., Mann, N., Buerger, F., Schneider, R., Deutsch, K., Kitzler, T. M., Klämbt, V., … Sanna-Cherchi, S. (2021). De novo TRIM8 variants impair its protein localization to nuclear bodies and cause developmental delay, epilepsy, and focal segmental glomerulosclerosis. *The American Journal of Human Genetics*, *108*(2), 357–367.

Wu, X., & Hurst, L. D. (2016). Determinants of the usage of splice-associated cis-motifs predict the distribution of human pathogenic SNPs. *Molecular Biology and Evolution*, *33*(2), 518–529.

Yamane, M., Sato, S., Shimizu, E., Shibata, S., Hayano, M., Yaguchi, T., Kamijuku, H., Ogawa, M., Suzuki, T., Mukai, S., Shimmura, S., Okano, H., Takeuchi, T., Kawakami, Y., Ogawa, Y., & Tsubota, K. (2020). Senescence-associated secretory phenotype promotes chronic ocular graft-vs-host disease in mice and humans. *The FASEB Journal*, *34*(8), 10778–10800.

Yang, S., Siepka, S. M., Cox, K. H., Kumar, V., de Groot, M., Chelliah, Y., Chen, J., Tu, B., & Takahashi, J. S. (2019). Tissue-specific FAH deficiency alters sleep-wake patterns and results in chronic tyrosinemia in mice. *Proceedings of the National Academy of Sciences of the United States of America*, *116*(44), 22229–22236.

SUPPORTING INFORMATION

Additional supporting information can be found online in the Supporting Information section at the end of this article.

How to cite this article: Chi, H., Gan, C., Jiang, Y., Chen, D., Qiu, J., Yang, Q., Chen, Y., Wang, M., Yang, H., Jiang, W., & Li, Q. (2023). The compound heterozygous mutations of c.607G>a and c.657delC in the *FAH* gene are associated with renal damage with hereditary tyrosinemia type 1 (HT1). *Molecular Genetics & Genomic Medicine*, *11*, e2090. https://doi.org/10.1002/mgg3.2090